

REPORT DOCUMENTATION PAGE			Form Approved OMB No. 0704-0188		
<p>The public reporting burden for this collection of information is estimated to average 1 hour per response, including the time for reviewing instructions, searching existing data sources, gathering and maintaining the data needed, and completing and reviewing the collection of information. Send comments regarding this burden estimate or any other aspect of this collection of information, including suggestions for reducing the burden, to Department of Defense, Washington Headquarters Services, Directorate for Information Operations and Reports (0704-0188), 1215 Jefferson Davis Highway, Suite 1204, Arlington, VA 22202-4302. Respondents should be aware that notwithstanding any other provision of law, no person shall be subject to any penalty for failing to comply with a collection of information if it does not display a currently valid OMB control number.</p> <p>PLEASE DO NOT RETURN YOUR FORM TO THE ABOVE ADDRESS.</p>					
1. REPORT DATE (DD-MM-YYYY) 08/___/2006		2. REPORT TYPE Technical Report		3. DATES COVERED (From - To) 6/1/04 - 5/31/06	
4. TITLE AND SUBTITLE Scaling of Energy Absorption in Composites to Enhance Survivability			5a. CONTRACT NUMBER NA		
			5b. GRANT NUMBER N00014-04-1-0326		
			5c. PROGRAM ELEMENT NUMBER 0601153N		
6. AUTHOR(S) Zdenek P. Bazant			5d. PROJECT NUMBER NA		
			5e. TASK NUMBER NA		
			5f. WORK UNIT NUMBER NA		
7. PERFORMING ORGANIZATION NAME(S) AND ADDRESS(ES) Northwestern University 2145 Sheridan Road Evanston, IL 60208-3109			8. PERFORMING ORGANIZATION REPORT NUMBER --		
9. SPONSORING/MONITORING AGENCY NAME(S) AND ADDRESS(ES) Office of Naval Research 875 N. Randolph St. Arlington, VA 22203			10. SPONSOR/MONITOR'S ACRONYM(S) ONR332 (Solid Mechanics Program)		
			11. SPONSOR/MONITOR'S REPORT NUMBER(S) NA		
12. DISTRIBUTION/AVAILABILITY STATEMENT Approved for Public Release; Distribution is Unlimited					
13. SUPPLEMENTARY NOTES					
14. ABSTRACT The objective of this paper is study the size effect on the nominal strength of imperfect sandwich structures for buckling driven delamination, to quantify this size effect, and to determine its intensity. A secondary objective is to assess the size effect on the postpeak energy absorption, important for judging survival under blast or dynamic impact. Buckling driven delamination is difficult to control in experiments. Thus, the present study relies on numerical simulations using geometrically nonlinear finite element analysis as well as the softening foundation model, which is an adaptation of Winkler elastic foundation. Delamination fracture is modeled by a cohesive crack model. Dimensionless variables are used to cover the entire practical range.					
15. SUBJECT TERMS Insert Key Words/Phrases (e.g., Sandwich Structures, Size Effects, Buckling,					
16. SECURITY CLASSIFICATION OF:			17. LIMITATION OF ABSTRACT UU	18. NUMBER OF PAGES	19a. NAME OF RESPONSIBLE PERSON Professor Zdenek P. Bazant
a. REPORT U	b. ABSTRACT U	c. THIS PAGE U			19b. TELEPHONE NUMBER (Include area code) 847-491-4025

Scaling of Energy Absorption in Composites to Enhance Survivability

ONR grant N00014-02-1-0622

PI: Z.P. Bažant, Northwestern University

Objectives and Approach: The technological objective (of ONR grant N00014-02-1-0622 "Fracture Scaling in Composites, Foams and Sandwich Structures", P.I. Z.P. Bažant) is to develop the scientific basis for designing efficient, reliable, light, affordable and terrorist-resistant structures and components of large high-performance ships as well as miniature devices important to naval warfare. The scientific objective is to determine the laws governing the scaling of quasibrittle or plastic failure important for large-scale behavior of composites (especially fiber composites) and their assemblies and components (rigid foams, sandwich structures for large ships, including hulls, decks, bulkheads, masts, protective covers, etc). The problem of scaling is approached through a combination of analytical and numerical studies with laboratory experiments.

Impact and Relevance to Navy: Mastery of scale effects, at present insufficient, would allow improved designs for large ships made mostly of composites, would improve terrorist-proof design and would also facilitate improvements of miniature devices for warfare.

Technology Transfer, Transitions: The knowledge gained in this project is being applied in a contract (joint with I. Daniel) with FAA to ensure safety of planned large load-bearing fuselage panel of Cirrus aircraft, and in a related PI's contract with Boeing Co. A collaboration with Prof. R. Vaziri of University of British Columbia is yielding further applications in safety evaluations of Boeing aircraft components.

SUMMARY:

For the design and performance of large ships static under dynamic as well as static loads, the energy absorption capability of the structure is of paramount importance. It depends on both the strength (or load capacity) and the steepness of post-peak softening of load versus deflection. For large quasibrittle structures, such as advanced ships built of fiber-polymer laminates and sandwich shells, knowledge of the scaling of both properties is of paramount importance of design, which inevitably depends on correct extrapolation of small-scale material properties to large sizes. Five fundamental problems of the scaling of strength and energy absorption of fiber composites and sandwich shells have been studied and significant results have been obtained. Five fundamental problems of the mechanics of fiber composites and sandwich shells have been studied and, for each of them, significant new findings have been achieved:

(1) A theoretical material constitutive law for laminates, accounting for cohesive fracture and damage localization, has been developed in the framework of the microplane theory.

(2) A novel experimental technique has been designed in order to capture the post-peak behavior of quasi-brittle composites; in this technique, the tensile softening behavior of a unidirectional carbon-epoxy laminate is stabilized by means of two layers of a glass-epoxy laminate capable of an ultimate strain larger than that of the carbon-epoxy.

20060906024

(3) Experiments on the size effect on failure loads of sandwich beams with PVC foam core and skins made of fiber-polymer composite have been conducted.

(4) Analysis of buckling and initial postbuckling behavior of soft-core sandwich structures, and soft-in-shear composites in general, has been analyzed.

(5) A previously unknown size effect on the type of probability distribution of strength of quasibrittle structures failing at crack initiation, implying size effect on safety factors in design, has been discovered and modeled theoretically.

EXTENDED SUMMARIES OF MAIN ACCOMPLISHMENTS:

(1) A complete solution of cohesive fracture and scaling model for sandwich skin debonding due to wrinkling instability has been obtained. So far, debonding has been analyzed by means of strength criteria or (rarely) by linear elastic fracture mechanics of sharp cracks, but this classical approach misses the size effect, the presence has been proven by PI's new experiments. Besides, the existing wrinkling formulas give only the elastic critical stress, but this stress is strongly modified by fracture. Also, mutually conflicting formulas, of unclear distinction among them, exist. These three problems were overcome by (i) coupling stability analysis with imperfections with cohesive fracture mechanics, characterized by finite fracture process zone in the interface, having both strength and energy limits; by (ii) distinguishing between long-wave and short-wave wrinkling; and by (iii) using a new asymptotic matching approach to "interpolate" between the last two. The result is a general wrinkling formula, of far broader applicability than the existing ones, which are included as special cases. The formula was verified by extensive geometrically nonlinear finite element fracture simulations.

(2) The first comprehensive material model for deformation and failure of fiber-polymer laminates has been developed, using the PI's microplane modeling approach in which the constitutive properties are expressed in terms of stress and strain vectors acting of a plane of generic orientation within the material ('microplane'), rather than in terms of stress and strain tensors and their invariants. In the existing formulations, separate disconnected models exist for elastic moduli as well as failure envelopes (such as Tsai-Wu), and nothing exists for fracture behavior and postpeak energy absorption, which are, therefore, ignored in design. To overcome this limitation, a nonlocal microplane constitutive model with fiber-generated orthotropy, based on softening stress-strain boundaries for planes of various orientations and on eigenmodes of stiffness matrix distinguishing longitudinal and transverse softening, has been developed. The model covers pre-peak hardening, strength envelopes and post-peak softening. The computational algorithm and the material identification procedure have been formulated, and the experimental stress-strain curves, failure envelopes, fracture data have been successfully matched. Since the existing experimental procedure could not capture, due to postpeak instability, the post-peak softening, a new type of test—the 'stabilized lamellar test' has been developed, in which the stress in softening of inner layer of lamellar specimens is inferred from different total load and the measured force in the stabilizing layer.

(3) The problem of stability of structures very weak in shear, such as the naval-type foam-laminate sandwich plates, has been solved. Various competing formulas have been subject to polemics for about 50 years. In small-strain situation, in which constant tangent elastic moduli ought to apply, they gave very different results for such structures. It was

found that while the critical load occurs at small strain, the tangent elastic moduli can be assumed to be constant for only one type of finite strain tensor, and that the type depends on the structure form and its loading. The consequence is that some known critical load equations, including the classical ones due to Biot as well as very recent ones, must be revised. A further result is that sandwich buckling is imperfection sensitive in certain important cases.

(4) The basics of the problem size effect in failure of naval type laminate-foam sandwich shells have been solved. So far, the size effect in sandwich strength has been unknown and ignored, yet the present research showed that it is significant for large structures such as navy ships. The existence of strong size effect was, *for the first time*, demonstrated by new types of scaled sandwich beam failure experiments, for both flexure and compression. Also, the size effect for sandwich beams was, *for the first time*, explained and predicted theoretically, by cohesive fracture mechanics of delamination fractures and cross-foam fractures. As a practical design tool, simple size effect equations for design have been developed.

(5) A previously unknown size effect on the type of probability distribution of strength of quasibrittle structures failing at crack initiation has been discovered and modeled theoretically. So far, the safety factors in design (about 1.5 to 2.0 for ships and aircraft) have been considered as empirical, and size independent. This assumption, implicit in all design so far, has been shown to be incorrect for quasibrittle failures, typical of laminates and sandwich structures. It has been found that the probability distribution of strength must be considered to be transitional between the Gaussian distribution (valid at small sizes) and Weibull distribution (valid at large sizes). These distributions have very different tails. A transitional strength distribution has been derived from nano-mechanics, based on the stress-sensitivity of the activations energy barriers of interatomic potential and on the Maxwell-Boltzmann distribution of atomic energies.

1. General Model for Sandwich Skin Delamination Due to Skin Wrinkling Instability with Imperfection and Cohesive Interface Fracture

A major question in extrapolating small-scale laboratory tests to full-scale sandwich structures is the size effect. Delamination of the skin (or facesheet) is often triggered by wrinkling instability, which has generally been considered to be free of size effect. The absence of size effect has been inferred from the fact that the critical stress for buckling generally exhibits no size effect. However, this inference is valid only for the symmetry-breaking bifurcation of equilibrium path in perfect structures. Actual sandwich structures are always imperfect at least to some degree, and often suffer dents from impacts which act as severe imperfections. Buckling of imperfect quasibrittle structures generally leads to snapthrough instability which typically exhibits size effect on the nominal strength.

Delamination in sandwiches and laminate composites has traditionally been analyzed by strength theory (either elasto-plasticity or elasticity with strength limit). This classical theory implies no size effect. However, according recent experiments by Bažant et al. [1] and Boyden et al. [2], the size effect in typical sandwich plates is transitional between the strength theory and linear elastic fracture mechanics. Therefore, the structure is quasibrittle, which means that the size of the fracture process zone (FPZ) cannot be

considered to be negligible to the cross section dimension of normal-size sandwich structures. So, delamination fracture is modeled by a cohesive crack model, rather than LEFM or strength theory.

The present study relies on numerical simulations using geometrically nonlinear finite element analysis as well as the softening foundation model, which is an adaptation of Winkler elastic foundation. Dimensionless variables are used to cover the entire practical range. Both shortwave and longwave wrinkling are considered.

Softening foundation model

The analysis of delamination in sandwich structures subjected to pure bending, as shown in Figure 1a, can be simplified by modeling the skin as an axially compressed beam supported by a softening foundation consisting of independent continuously distributed nonlinear springs Figure 1b. For the mathematically analogous problem of a foundation with bilinear elastic-plastic hardening response, the solution is available [3]. Here the problem is solved for bilinear elastic-softening response, in which the softening represents gradual decohesion due to a cohesive crack under the beam. The differential equation of the problem reads

$$E_s I_s \frac{d^4 W}{dX^4} + P \frac{d^2 W}{dX^2} + F = -P \frac{d^2 W^o}{dX^2} \quad (1)$$

where E_s is the Young's modulus of the skin, $I_s = t^3/12$ is the moment of inertia (per unit width) of the cross section of the skin of thickness t , P is the axial force in the beam (per unit width), X in the coordinate in the axial direction and $W(X)$ is the deflection (lateral displacement) of the skin, additional to the initial deflection W^o .

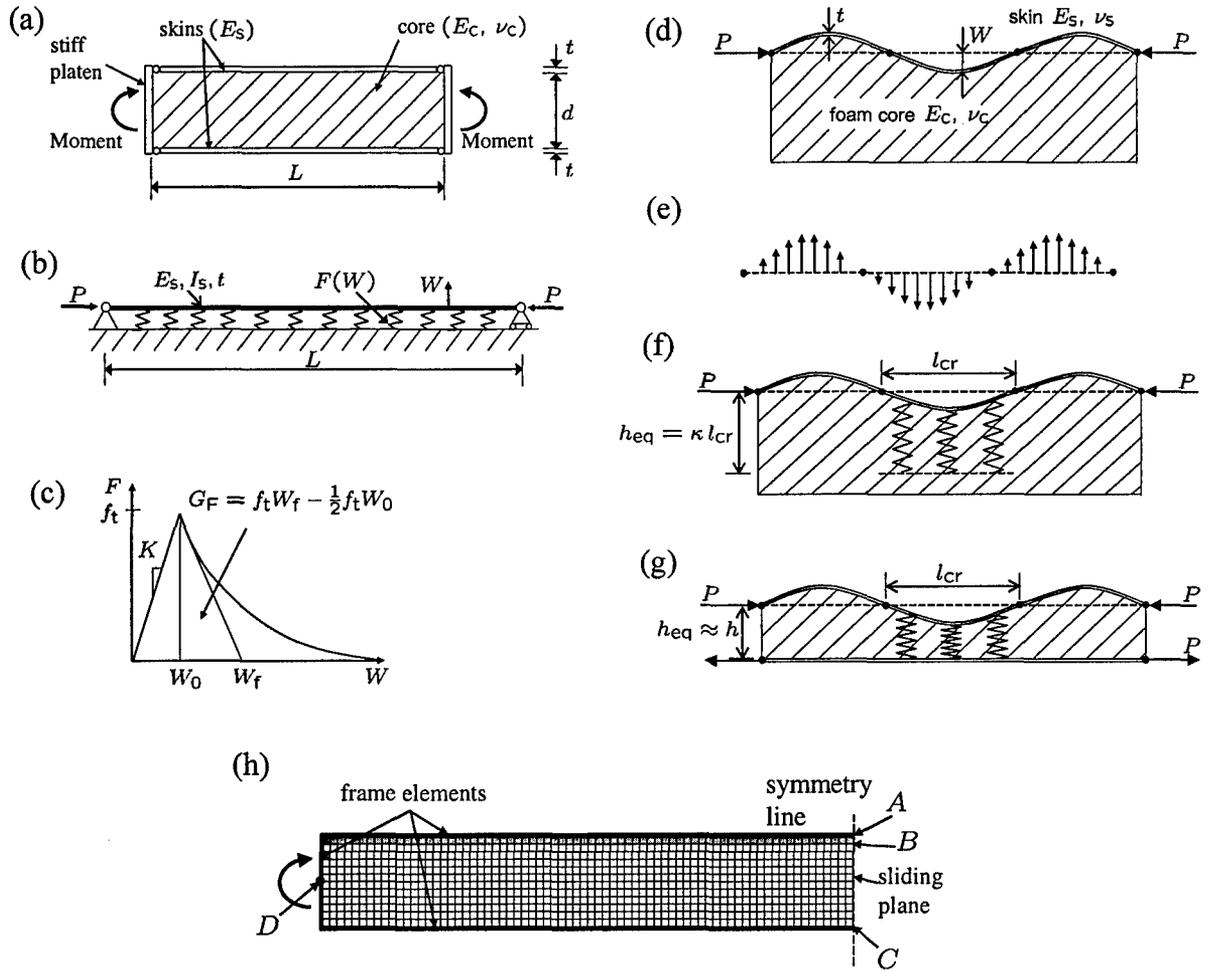


Figure 1: (a) The geometry of a typical sandwich beam subjected to pure bending. (b) The beam subjected to an axial compression force P supported by a softening foundation. (c) The force-displacement relation of the softening foundation. (d) The deflection of the top skin. (e) Equilibrated stress acting on the foam. (f) Equivalent height for shortwave and (g) longwave wrinkling. (h) The finite element mesh.

Furthermore, F is the distributed lateral force (traction), defined as

$$F = \begin{cases} KW & \text{if } W \leq W_0 \\ KW_0 e^{-(W-W_0)/(W_f-W_0)} & \text{if } W > W_0 \end{cases} \quad (2)$$

where K is the foundation modulus (i.e., the spring stiffness of the foundation per unit length), W_0 is the displacement at which the tensile strength f_t is reached (Figure 1c).

$$G_F = f_t(W_f - W_0/2) \quad (3)$$

G_F represents the area under the stress-displacement curve in Figure 1c. The distributed spring stiffness K (per unit length of the beam) may be interpreted as

$$K = E_c / h_{eq} \quad (4)$$

Where E_c is Young's modulus of the sandwich core, and h_{eq} represents the equivalent (or effective) depth of the foundation.

For **shortwave wrinkling** the wave length $L_{cr} \ll h$ (h = core thickness). In that case the core may be regarded as an infinite half space. The reason is that the alternating tractions applied on the core by the periodically wrinkled skin (Figure 1e) are self-equilibrated over a segment of length $2L_{cr}$ where L_{cr} is the half-wavelength of the skin buckling (Figure 1f). Therefore, according to the Saint-Venant principle, the stresses caused by periodic wrinkling must exponentially decay to nearly zero over a distant from the skin roughly equal to $2L_{cr}$. Therefore, it must be possible to write

$$h_{eq0} = \kappa L_{cr} \quad (5)$$

where κ is some constant and subscript 0 refers to the limit case $L_{cr}/h \rightarrow 0$.

This leads to an expression for the critical axial compression force in the skin at bifurcation (see Bažant and Grassl [4] for details) as

$$P_{cr0} = 2\sqrt{KE_s I_s} = k_1 \left(E_c'^2 E_s \right)^{1/3} t \quad \text{where} \quad k_1 = \left(2/3\kappa^2 \pi^2 \right)^{1/3} \quad (6)$$

Note that this expression has the same form as derived in Hoff and Mautner [5], if $\kappa = \alpha\sqrt{1+\nu_c}$ with $\alpha = 0.43$. Here, however, $\alpha = 0.53$ is used, as determined from a single finite element analysis.

Consider now the case of **longwave wrinkling** ($L_{cr} \gg h$), shown in Figure 1g, and that the sandwich beam is subjected to bending moment only (i.e. with no axial force). Then the opposite skin is under tension and may be approximated as rigid base, with no deflection. The transverse compressive stress in the core is now almost uniform, and

$$h_{eq\infty} = h \quad (7)$$

i.e., the foundation stiffness $K = E_c' / h_{eq}$ is constant (independent of the critical wavelength). The critical compressive force in the skin at bifurcation for periodic skin buckling (without delamination) is

$$P_{cr\infty} = 2\sqrt{KE_s I_s} = \sqrt{E_c' E_s t^3 / 3h} \quad (8)$$

where subscript ∞ refers to the limit case $L_{cr}/h \rightarrow \infty$, for which the solution is exact. The same expression was reported in Heath [6].

The **transition** between shortwave and longwave wrinkling is smoothly distributed over a certain dimensionless variable

$$\zeta = h_{eq0} / h \quad (9)$$

The shortwave bound $h_{eq} = h_{eq0}$ must be tangentially approached for $\zeta \rightarrow 0$, and the longwave bound $h_{eq} = h_{eq\infty}$ must be an asymptote for $\zeta \rightarrow \infty$.

An expression that meets all the asymptotic conditions is

$$h_{eq0} / h_{eq} = \zeta + e^{-(\zeta + a_1 \zeta^2 + a_2 \zeta^3)} \quad (10)$$

where $a_1 = 0.24$ and $a_2 = 0.36$, as obtained by fitting to linear elastic finite element results with the Marquardt-Levenberg algorithm for nonlinear least-squares optimization.

Formulation in Dimensionless Variables

The solution may generally be expressed as a relation among seven dimensional variables: $E_s I_s, K, P, W_0, W^0, W_f, x$ which involve 2 independent dimensions, force and length. According to Vashy-Buckingham theorem of dimensional analysis, the number of dimensionless variables governing the problem is $7 - 2 = 5$. They may be chosen the same as in a previous study of plastic bilinearly hardening foundation [3]:

$$x = X(E_s I_s / K)^{-1/4}, \lambda = \frac{1}{2} P (K E_s I_s)^{-1/2}, w = W / W_0, w^0 = W^0 / W_0, w_f = W_f / W_0 \quad (11)$$

Substituting these equations and Eq. (2) in Eq. (1), yields the dimensionless differential equation:

$$\frac{d^4 w}{dx^4} + 2\lambda \frac{d^2 w}{dx^2} + w = -2\lambda \frac{d^2 w^0}{dx^2} \quad \text{if } w \leq 1 \quad (12)$$

$$\frac{d^4 w}{dx^4} + 2\lambda \frac{d^2 w}{dx^2} + e^{(w-1)/(w_f-1)} = -2\lambda \frac{d^2 w^0}{dx^2} \quad \text{if } w > 1 \quad (13)$$

where w is the dimensionless deflection. For a perfect beam ($w^0 = 0$), the first eigenmode of buckling at bifurcation is determined from Eq. (12) as $w = \sin x$, and the corresponding load at bifurcation results in $\lambda = 1$. A general imperfection of skin may be expressed as a combination of all eigenmodes of buckling. The first eigenmode may be expected to have dominant influence. Therefore, the imperfection δ of the skin is chosen to be proportional to the aforementioned displacement profile $w = \sin x$ of a perfect skin at first bifurcation, i.e. $w^0 = \delta \sin x$. The solution of (1) for the elastic case ($w_{\max} < 1$), with the aforementioned imperfection, is

$$w(x) = \frac{\lambda \delta}{1 - \lambda} \sin x \quad (14)$$

The solution will be used for deriving the size effect law.

The dimensionless variables x, w, w^0 and λ are size independent. However, ensuring constant fracture energy (in the sense of the crack band model) requires that the dimensionless parameter w_f be considered size dependent, as obtained by inserting (3) into (11);

$$w_f = \frac{G_F E_c}{f_t^2 h_{eq}} + \frac{1}{2} \quad (15)$$

Parameters G_F, E_c and f_t are material properties independent of the structure size, while h_{eq} is proportional to the structure size. Thus, the size dependence of w_f can be characterized as

$$w_f = \frac{1}{\xi} + \frac{1}{2} \quad (16)$$

where

$$\xi = h_{eq} / l_0, \quad l_0 = E_c G_F / f_t^2 \quad (17)$$

ξ is dimensionless and l_0 is known as Irwin's characteristic material length, approximately characterizing the fracture process zone length. To simplify analysis, only one half of the beam is modeled and symmetric deformation is assumed.

Geometrically nonlinear finite element analysis

To determine parameter α and to validate the simplified modeling of delamination by the softening foundation model, a geometrically nonlinear finite element program (FEAP) is used. A sandwich beam, depicted in Figure 1a, is considered and is modeled using the finite element mesh in Figure 1h. The skins are represented by beam elements taking into account large displacements and large rotations. For the core, plane stress finite elements based on a linearized small displacement formulation is used. The core is treated as isotropic, and for the skin only the longitudinal elastic modulus E_s needs to be considered since the transverse and shear moduli of laminate skin are immaterial for bending and axial deformation.

The beam is considered to be subjected to a uniform bending moment, M . However, as long as the core thickness h is large enough for the stresses from wrinkling to decay to nearly zero over the core thickness, the only loading that matters is the axial force. Whether this force is produced by moment alone, or a combination of bending moment and axial force, is immaterial.

An elastic stress-strain relation is used for all the elements of the core except a narrow band of elements under the skin (marked gray in Figure 1h). It is known that the delamination fracture occurs within the core very near the interface with the skin, but not within the interface. Therefore, perfect bond between the skins and the core is enforced. Transverse softening of the aforementioned band, which can be regarded as distributed microcracking, simulates delamination. In the softening band, the stress-strain law is elastic in the pre-peak, and the post-peak response follows the isotropic damage model, which is defined as

$$\sigma = (1 - \omega) D_c : \varepsilon \quad (18)$$

Here σ and ε are the stress and strain tensors in the core, ω is the damage variable, and D_c is the isotropic elastic stiffness tensor of the core, which is based on the Young's modulus E_c and the Poisson's ratio ν_c . The damage law is chosen so that it results in an exponential stress-strain curve in uniaxial tension. The inelastic strains determined by the isotropic damage model are fully reversible, i.e. the secant stiffness points toward the origin (this reversibility would, of course, be unrealistic if crack unloading were not nonexistent in the present simulations).

As before, only half of the beam is modeled. The loading moment M is applied at point D (Figure 1h) and is assumed to be transferred by a rigid loading platen into the upper and lower skins. The structure is restrained in longitudinal direction at point A . The loading is controlled by prescribing the displacement of point B . The same initial displacement, i.e. $w^0 = \delta \sin x$, is prescribed for the upper skin. The imperfection amplitude at the middle of the beam at point A is slightly increased in the same way as for the softening foundation model, to control the place where the delamination begins.

Results and comparison of softening foundation to finite elements

The effect of the structure size on the relation between the load parameter λ and the mid-point displacement $w_a = w(L/2)$ is shown, for three imperfection amplitudes $\delta = 0.1, 1, 2$, in Figure 2a-c. As one can see, the results of the softening foundation model are in reasonable approximate agreement with the more accurate finite element results. The comparison shows that the size has a strong effect on the post-peak part of the load-displacement relation. The larger the size, the less energy is dissipated in relation to the

energy dissipated by delaminating the entire skin. Furthermore, a closer examination of the size effect on the evolution of the diagram of load versus blister length (which is the length in the middle portion of the beam in which $w > 1$) reveals a size effect on the nominal strength, see Figure 2d-f. The larger the size, the smaller is λ_{\max} . Furthermore, note that the size effect intensity depends strongly on the imperfection amplitude. A law for this size effect is proposed next.

Size effect law for imperfection sensitive wrinkling

The size effect on the dimensionless nominal strength, $\lambda_N = \lambda_{\max}$, shown in Figure 2g, has a form similar to the size effect law for crack initiation in quasibrittle structures proposed by Bažant [7,8]. This law, however, is not directly applicable since imperfections are seen in Figure 2g to influence the size effect. Therefore, a generalized law of the form

$$\lambda_N(\delta, \xi) = \lambda_\infty(\delta) \left[1 + \frac{1}{k(\delta) + a\xi^b} \right], \quad k(\delta) = c\delta^{-d} \quad (19)$$

is proposed here, with constants a, b, c, d and parameters λ_∞ and k depending on the imperfection amplitude δ . For large sizes ($\xi \rightarrow \infty$), the nominal strength is decided by crack initiation ($w = 1$), and in that case Eq. (19) leads to

$$\lambda_N(\delta, \infty) = \lambda_\infty = 1/(1 + \delta) \quad (20)$$

For small sizes ($\xi \rightarrow 0$), the nominal strength in (19) turns into

$$\lambda_N(\delta, 0) = \lambda_\infty(\delta) \left[1 + \frac{1}{k(\delta)} \right] \quad (21)$$

Parameters a, b, c, d in Eq. (19) are determined as optimal fits of numerical results using the Marquardt-Levenberg algorithm for nonlinear least-squares optimization. First the parameters c and d are determined from the fit of the results for the smallest size ($\xi = 0.001$) in Figure 2g, for varying imperfections. Then the parameters a and b in Eq. (19) are fitted for the largest imperfection ($\delta = 6$) and varying size. The optimum values are $a = 9.94$, $b = 1.2$, $c = 6.82$, $d = 1.21$. The size effect law in Eq. (19) using these parameters is compared to the results of the softening foundation model in Figure 2g. The approximation is seen to be satisfactory.

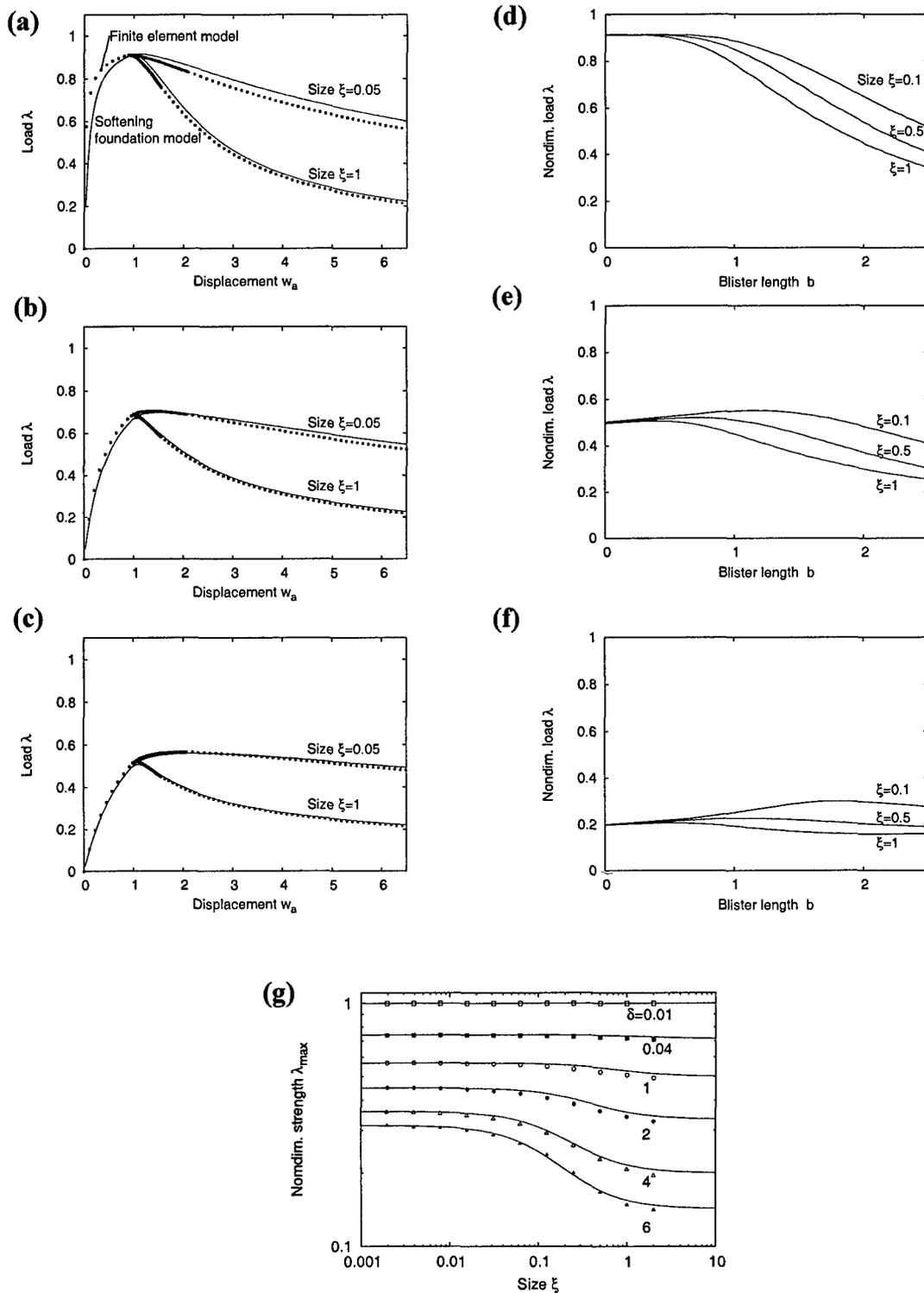


Figure 2: (a)-(c): The load λ versus the mid-point displacement w_a obtained with the softening foundation model and the finite element model for the imperfections (a) $\delta = 0.1$, (b) $\delta = 0.5$, (c) $\delta = 1$ for two sizes ($\xi = 1$ and $\xi = 0.05$). (d)-(f): The load λ versus the blister length (mid beam region in which $w > 1$) of the upper skin for the imperfections (d)

$\delta = 0.1$, (e) $\delta = 1$, (f) $\delta = 4$. (g) Comparison of the size effect law with the nominal strength-size relations obtained with the softening foundation model for different imperfections.

Conclusions

1. In view of recent experiments revealing a size effect transitional between LEFM and strength theory, the delamination fracture of laminate-foam sandwich structures must be treated as a cohesive crack with a softening stress-separation relation characterized by both fracture energy and tensile strength. In contrast to LEFM, no pre-existing interface flaw needs to be considered.

2. The skin (or facesheet) can be treated as a beam on elastic foundation, provided that the equivalent (or effective) core depth h_{eq} for which the hypothesis of uniform transverse stress gives the correct foundation stiffness is considered to depend on the critical wavelength L_{cr} of skin wrinkles; $h_{eq} = h$ for the asymptotic case of longwave wrinkling ($L_{cr}/h \rightarrow \infty$), while (because of St. Venant principle) h_{eq} is proportional to L_{cr} for the asymptotic case of shortwave wrinkling ($L_{cr}/h \rightarrow 0$).

3. A properly formulated softening foundation model can give good agreement with geometrically nonlinear finite element analysis of delamination fracture triggered by wrinkling.

4. Although the nominal strength of sandwich structures failing by wrinkling-induced delamination fracture is size independent when there is no imperfection, it becomes strongly size dependent with increasing imperfection.

5. Introduction of proper dimensionless variables makes it possible to cover with numerical simulations the entire practical range, and fitting the dimensionless numerical results for cohesive delamination fracture with a formula for correct shortwave and longwave asymptotics allows constructing an approximate size effect law for nominal strength of arbitrarily imperfect sandwich beams subjected to uniform bending moment.

6. There is also a strong size on postpeak energy absorption by a sandwich structure, both in presence and absence of imperfections. This is important for impact and blast resistance.

2. Comprehensive Microplane Model for Non-Linear Behavior, Strength Envelopes, Fracture and Postpeak Energy Absorption of Laminates

A novel microplane model has been developed to represent the energy absorption in postpeak softening behavior of fiber composites envisaged for use in proposed large Navy ships. This model is capable of capturing not only prepeak but also postpeak nonlinearity, particularly the material softening due to cracking damage of laminates, which, in turn, leads to the possibility of a comprehensive model for predicting the size effect in static failures and the energy absorption capability under dynamic loading, such as impact, blast or shock.

The microplane model is a modification of the classical Taylor's idea conceived by Bažant and already developed for several other materials (concrete, rock, soil, polymeric foam, polycrystalline metals). In this model, the use of tensors and their invariants is bypassed by formulating the constitutive law as a relation between the stress and strain vectors on generic planes in the material, called the microplanes. The responses from the microplanes of all possible orientations are then combined according to a variational principle to obtain the response of the

macroscopic continuum. In the case of softening damage, this must be done under a kinematic (rather than static) constraint, in which it is assumed that the strain vectors on all the microplanes are the projections of the macroscopic strain tensor.

Compared to typical isotropic materials, a great modeling difficulty for composites is presented by their anisotropy. In the present study, the anisotropic microplane model in a novel way which exploits the spectral decomposition of the 6×6 stiffness matrix \mathbf{E} and reads:

$$\mathbf{E} = \sum_{I=1}^6 \lambda_I \mathbf{E}_I \quad (1)$$

where λ_I are the eigenvalues of the stiffness matrix and \mathbf{E}_I define a set of orthogonal matrices constructed from the eigenvectors of \mathbf{E} , respectively. In the isotropic case, the spectral decomposition exactly coincides with the volumetric-deviatoric decomposition already used in the formulation of the microplane model for isotropic materials.

The matrices \mathbf{E}_I decompose the strain tensor (represented in Voigt's notation) into orthogonal strain modes $\boldsymbol{\varepsilon}_I = \mathbf{E}_I \boldsymbol{\varepsilon}$. Each strain mode can then be projected into a generic microplane to define a set of orthogonal measures of normal and shear strains: $\boldsymbol{\varepsilon}_{PI} = \mathbf{P}_I \boldsymbol{\varepsilon}$, where $\mathbf{P}_I = \mathbf{P} \mathbf{E}_I$, \mathbf{P} is a linear operator transforming the usual continuum strains (ε_{ij}) into microplane strains ($\varepsilon_N, \varepsilon_M, \varepsilon_L$), and $\boldsymbol{\varepsilon}_{PI} = [\varepsilon_{NI} \ \varepsilon_{MI} \ \varepsilon_{LI}]^T$.

In the elastic regime the microplane stress vectors $\boldsymbol{\sigma}_{PI} = [\sigma_{NI} \ \sigma_{MI} \ \sigma_{LI}]^T$ can be computed as $\boldsymbol{\sigma}_{PI} = \lambda_I \boldsymbol{\varepsilon}_{PI}$. In the inelastic regime, instead, the normal (σ_{NI}) and shear ($\sigma_{TI} = [\sigma_{MI}^2 + \sigma_{LI}^2]^{1/2}$) stress components are restricted by the stain-softening boundaries:

$$\sigma_{Nbl}^-(\boldsymbol{\varepsilon}_I^-) \leq \sigma_{NI} \leq \sigma_{Nbl}^+(\boldsymbol{\varepsilon}_I^+); \quad \sigma_{Tbl}(\boldsymbol{\varepsilon}_I^-, \boldsymbol{\varepsilon}_I^+) \leq \sigma_{TI} \leq \sigma_{Nbl}(\boldsymbol{\varepsilon}_I^-, \boldsymbol{\varepsilon}_I^+) \quad (2)$$

The macroscopic stress tensor can be then obtained by the Principle of Virtual Work, which reads:

$$\boldsymbol{\sigma} = \frac{3}{2\pi} \int_{\Gamma} \mathbf{P}_I^T \boldsymbol{\sigma}_{PI} d\Gamma \quad (3)$$

The present formulation has been applied to the simulation of the behavior of unidirectional laminates. Figure 3 shows the comparison between experimental (red points) and numerical (black line) stress-strain curves of a unidirectional carbon-epoxy laminate under tension (fiber direction on top left and transverse direction on top right), compression (bottom left), and shear (bottom right). The agreement up to the peak is very good. In the post-peak regime, no experimental results exist and further study will be required. In particular, a new experimental technique able to capture the post-peak behavior of laminates is needed. It will be discussed in the next section.

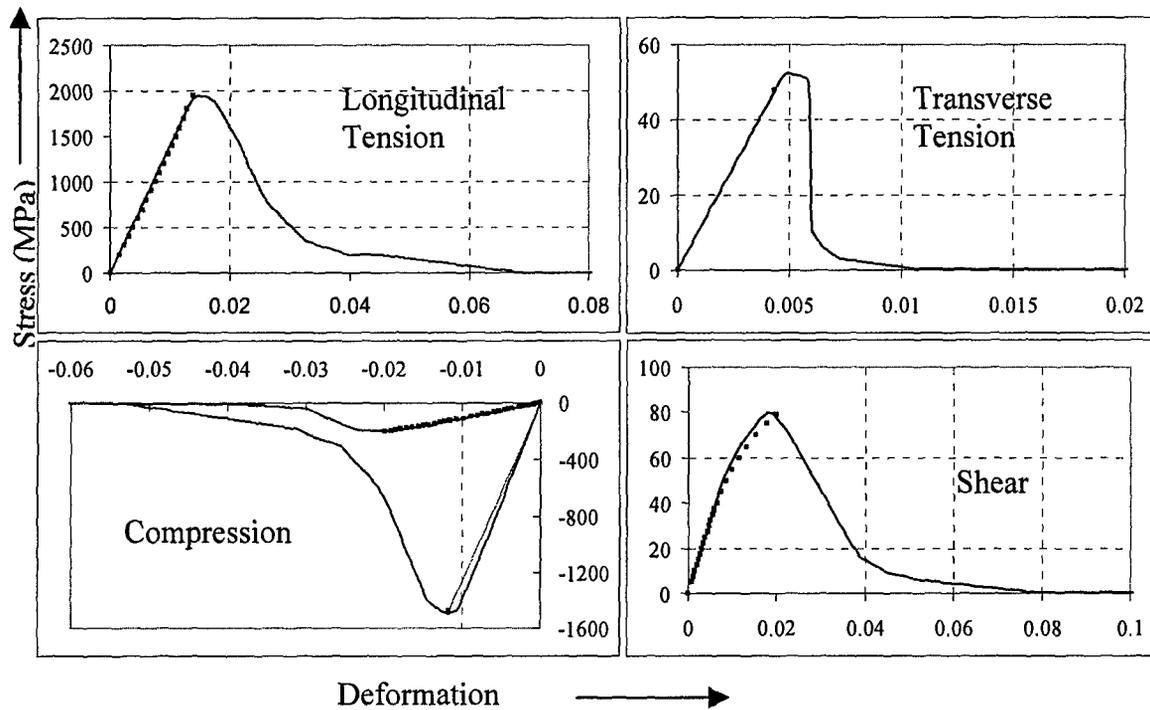


Figure 3: Microplane model simulation of a unidirectional laminate under uniaxial loading

Figure 4 shows the comparison between the experimental (blue points) and numerical (red line) failure envelopes obtained by applying simultaneously shear and normal stress in the direction of the fiber (left) or shear and normal stress transversely to the fiber (right). In the figure the very well known Tzai-Wu criterion also appears for comparison (green line).

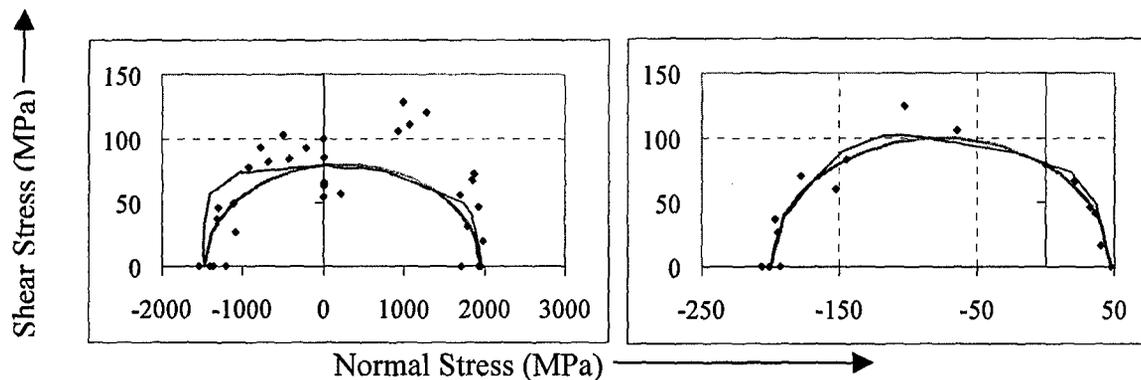


Figure 4: Microplane model simulation of biaxial failure envelope of a unidirectional laminate.

3. Size Effect in Failure of Sandwich Structures

Experiments have been conducted on sandwich beams of different sizes, consisting of fiber composite skins and a vinyl foam core, in order to investigate in detail the scaling of failure loads. The cores of all sandwich beams were made of closed cell polyvinylchloride (PVC) foam with mass density 100 kg/cm^3 . The properties of the foam were as follows: tensile elastic modulus 105 MPa, tensile strength 3.1 MPa, compressive elastic modulus 125 MPa, compressive strength 1.7 MPa, elastic shear modulus 40 MPa, and shear strength 1.4 MPa.

Three series of tests were carried out, named series I, II and III. The beams manufactured were geometrically scaled in two dimensions, maintaining the same width $b = 25.4$ mm. The thickness t of the skins too was scaled in proportion to the core depth c . The scaling ratios were 1:4:16 for series I and 1:3:9 for series II and III. For series III, the beams had no notches. For series I and II, notches were cut in the foam as close as possible to the top or bottom skin, respectively, but without cutting into the skin. The notches in series I and II were symmetric, cut from both ends of the beam. The distance a of each notch tip from the support axis was equal to core depth c . The notches were made in order to clarify the effect of large pre-existing cracks or damage zones, and to force the fracture to develop at a certain pre-determined location, homologous (geometrically similar) for all the sizes. The notches also helped avoiding a conceivable Weibull-type statistical contribution to the size effect. All the beams were subjected to three-point bending.

The skins of the test series I consisted of woven glass fiber-epoxy composite. Figure 8 (left) shows the typical records of the load-deflection curves for all three sizes. It is obvious that, the larger the specimen, the more brittle its response. The measured values of nominal strength $\sigma_N = P/(bD)$ are plotted in Figure 8 (right). The figure shows an anomalous size effect characterized by a positive curvature. This anomaly could be attributed to the compression in the top skin and to the interaction of mode II fracture propagation with skin wrinkling instability in compression.

Therefore, a second test series (series II) was carried out, with notches near the bottom skin, which is in tension.

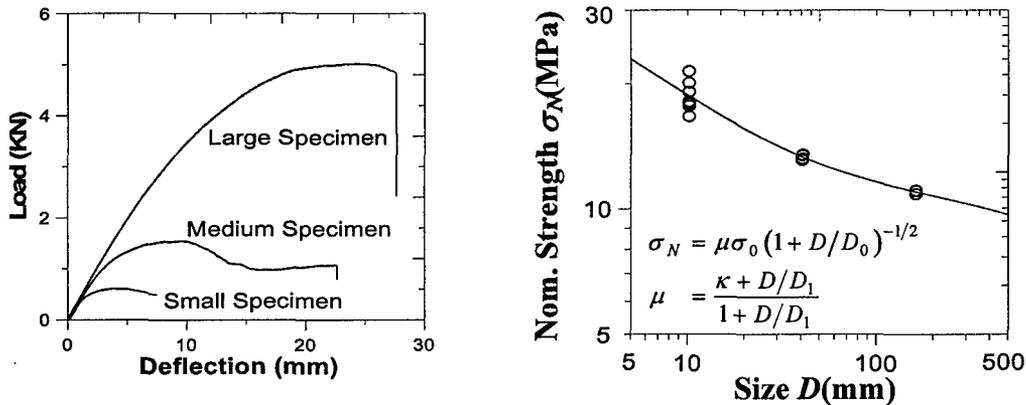


Figure 5: Load-deflection curves for series I specimen (on the left) and nominal strength (on the right). The solid curve on the right represents the prediction by modified Bažant's size effect law (SEL).

The skins for this series were made of a carbon-epoxy laminate. Without exception, all the specimens failed by diagonal tensile fractures which propagated through the foam from the notch tips (Figure 6 top). Also for this test series the largest specimens exhibited a more brittle behavior. Figure 6 shows the load-deflection curves (bottom left) and the values of nominal strength (bottom right).

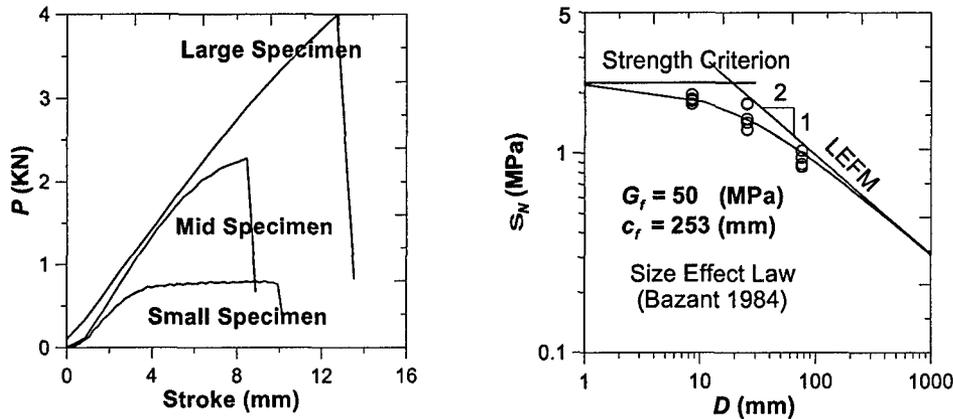
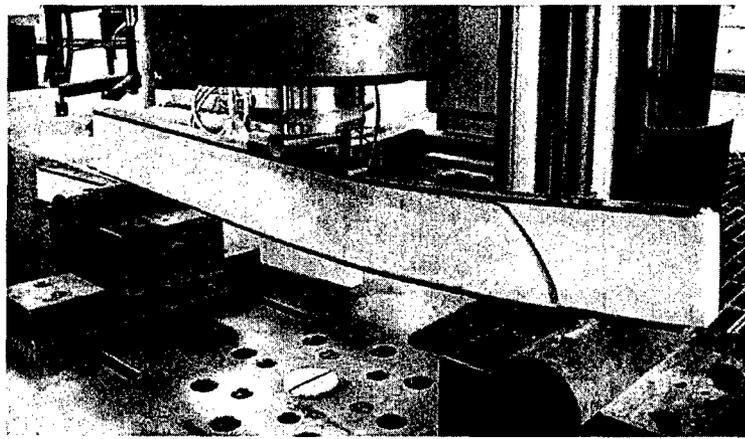


Figure 6: Typical failure for the specimens of series II (top). Load-deflection curves for series II specimens (bottom left) and nominal strength (bottom right). The solid curve represents Bazant's SEL.

The beams of test series III were the same as in series II, except for the foam block dimensions and the absence of notches. In the small beams, no diagonal shear fracture was observed; rather, the failure was caused by compressive fracture of the upper skin. This mode of failure was also observed in some medium and large beams, but in most of these beams the interface crack branched into a diagonal tensile crack, which crossed the foam core.

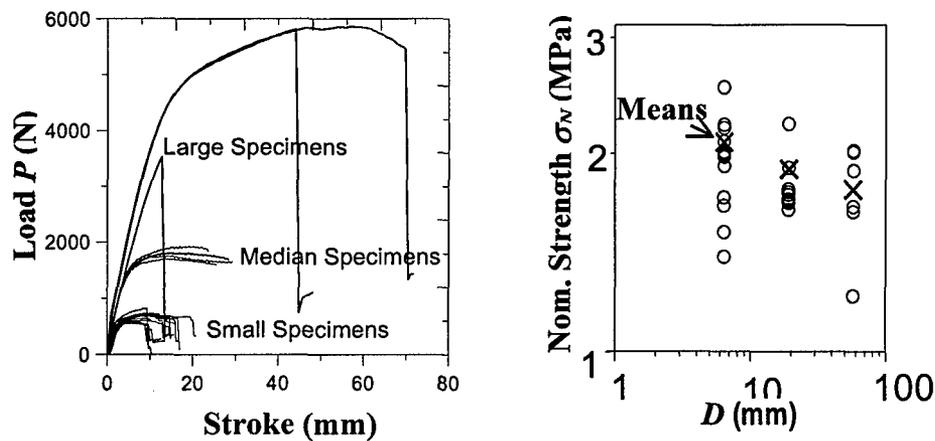


Figure 7: Load-deflection curves for series III specimen (on the left) and nominal strength (on the right).

A significant size effect was found again, but it was not as strong as in notched beams. The load-deflection curves for the beams of all three sizes are shown in Figure 7 (left), and the values of nominal strength are plotted in Figure 7 (right).

The experimental results emphasize a significant size effect, which cannot be attributed to the Weibull-type statistical size effect since, in the notched as well as unnotched beams tested, the crack always propagated from the same location and not from a random one. Besides, the mean nominal strength depicted in Figure 7 (right) shows a deviation from linear elastic fracture mechanics (LEFM), which makes the use of LEFM for calculating load capacity unrealistic.

These results show, on one hand, that the common engineering practice of predicting the load capacity of sandwich structures based upon the concept of material strength or plastic limit analysis is incorrect and needs to be revised, and on the other hand, that failure theories with a characteristic length, such as fracture mechanics based on the cohesive crack model, crack band model or nonlocal damage mechanics, must be applied. This is particularly important for large naval structures of sandwich construction.

Size Effect on Compressive Strength of Laminate-Foam Sandwich Plates

Prismatic sandwich specimens of various sizes, geometrically scaled in the ratio 1 : 2 : 4 : 8, are subjected to eccentric axial compression and tested to failure. The sandwich core consists of a closed-cell PVC foam, and the facesheets are woven glass-epoxy laminates, scaled by increasing the number of plies. The test results reveal a size effect on the mean nominal strength, which is strong enough for requiring consideration in design. The size effect observed is fitted with the size effect law of the energetic (deterministic) size effect theory. However, because of inevitable scatter and limited testing range, the precise form of the energetic size effect law to describe the test results is not unambiguous. The Weibull-type statistical size effect on the mean strength is ruled out because the specimens had small notches which caused the failure to occur in only one place in the specimen, and also because the observed failure mode was kink band propagation, previously shown to cause energetic size effect. Various fallacies in previous applications of Weibull theory to composites are also pointed out.

New Experiments to Characterize Post-Peak Softening in Laminates

Preliminary tensile failure experiments have been carried out to supplement previous indirect test evidence by directly calibrating the diverse parameters of the microplane model, in particular the post-peak tensile softening region. A new testing method, called the *lamellar test*, has been devised to stabilize the behavior of a laminate in postpeak softening (see Figure 8 for a sketch of the experiment). The idea is to bond two stiff plates with very high strain at elastic limit to both sides of a tensile specimen to be tested, then record the load-deflection response of this combined specimen, and to deduce from it the stress in the laminate as the difference between the measured overall stress and the stress carried by the bonded stabilizing plates. With a different purpose, test data relevant to this idea have already been obtained for cross-ply laminates, for which the stabilizing plates consisted of very stiff outer 0° layers. However, tests of the softening behavior of a laminate loaded in the fiber direction were never carried out before.

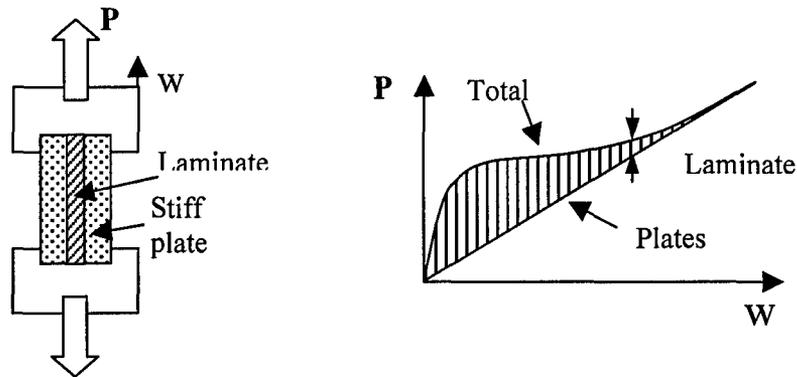


Figure 8 : Lamellar test for postpeak behavior and load-deflection curves from which the softening law can be extracted

The preliminary tests carried out on carbon-epoxy specimens stabilized by means of glass-epoxy plates were not able to capture the softening region because the specimens experienced a sudden dynamic failure immediately after reaching the peak stress in the carbon-epoxy layer (see Figure 9). This problem was caused by insufficient stiffness of the available testing machine, which was not large enough compared to the stiffness of the specimen. Currently, several types of alloys are considered as possible candidates to reinforce the outer glass-epoxy plates in order to stabilize the specimen behavior in the softening regime. In that way it should be possible to measure the complete softening curve in such tests, and obtain from it both the material fracture energy and the material characteristic length l .

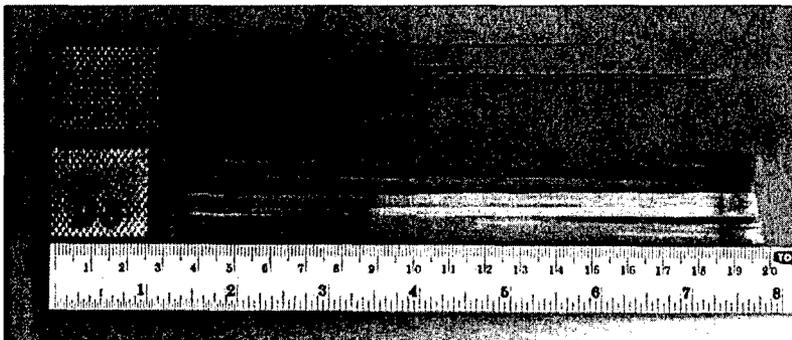


Figure 9: One of the lamellar specimens after the test

4. Shear Buckling and Initial Postbuckling of Fiber Composites and Sandwich Structures

The critical load of columns deflecting with significant shear deformations like sandwich columns and composite columns is not unambiguous. Two very different theories are well known--Engesser's theory (Engesser 1889, 1889a, 1891), in which the shear deformation is considered to be caused by the shear force in a cross section normal to the deflection curve, and Haringx's theory (Haringx 1942, 1948), in which the shear deformation is considered to be caused by the shear force in a cross section that was normal to the beam axis in the original un-deflected configuration.

In the research conducted under this grant in the preceding year, it was proven that if the initial strains and stresses are so small that all the material remains in the linear range, a constant tangent (or incremental) shear modulus G for the case of sandwich structures can be used only with the Engesser-type theory, and that the Haringx-type theory is usable only if G of the core is

considered to be a linear function of the axial stress in the skins. In addition, it was shown that finite element predictions of commercial softwares are in agreement with the critical load given by the Engesser-type formula. The reason for this agreement is that the updating algorithm assumes the material moduli tensor as constant with respect to the Lagrangian coordinates during each loading step.

In the last year of study under this grant, the consequences of this previous research were explored for the case of general homogenized orthotropic structures very soft in shear, including layered structures that are loaded transversely to the direction of stiffening plates, and structures loaded in both directions of orthotropy. In addition, the initial postbuckling behavior of sandwich and fiber composite structures has been explored to understand the effect of imperfection sensitivity, which causes the structures to reach a maximum during loading and then to soften. It has been discovered that structures weak in shear for certain combination of material stiffnesses may show this type of behavior, which has to be taken into account in design.

Soft-in-Shear Fiber Composites and Layered Bodies Under Initial Biaxial Stress

First, let us recall the class of Doyle-Ericksen finite strain tensors $\boldsymbol{\varepsilon} = (\mathbf{U}^m - \mathbf{I})/m$ (where m = real parameter, \mathbf{I} = unit tensor, and \mathbf{U} = right-stretch tensor), which include virtually all the strain measures ever used in the literature. The stability criteria expressed in terms of any of these strain measures are mutually equivalent if the tangential moduli associated with different m -values satisfy Bažant's (1971) relation:

$$C_{ijkl}^{(m)} = C_{ijkl} + \frac{1}{4}(2-m)(S_{ik}S_{jl} + S_{jk}S_{il} + S_{il}S_{jk} + S_{jl}S_{ik}) \quad (4)$$

where subscripts refer to Cartesian coordinates x_i , $i = 1, 2, 3$, C_{ijkl} = tangential moduli associated with Green's Lagrangian strain ($m = 2$), and S_{ij} = current stress (Cauchy stress).

Let us now consider the homogenized continuum in Figure 10 to deform in the plane (x_1, x_3) and to be initially subjected to finite initial normal stresses S_1^0 and S_3^0 in the directions parallel and normal to the plates or fibers (see Figure 10). A unit width in the x_2 direction is considered. The incremental displacements are given by u_1 and u_3 , while $\gamma = \theta - \psi$ is the shear angle where $\theta = w' =$ slope of the deflection curve. Clearly, a sandwich column is a special extreme case for initial stresses $S_1^0 = 0$ and $S_3^0 = -P/h < 0$. The incremental second order work per unit volume is:

$$\begin{aligned} \delta^2 W &= \frac{1}{2}G\gamma^2 + \frac{1}{bh} [S_1^0 b(h - AB'' \cos \vartheta) + S_3^0 h(b - AC' \cos \psi)] \\ &\approx \frac{1}{2}G\gamma^2 + \frac{S_1^0}{2}(u_{3,1}^2 - \gamma^2) + \frac{S_3^0}{2}u_{1,3}^2 \end{aligned} \quad (5)$$

The above expression must be equal to the second order work of the homogenized continuum (see the references for details):

$$\delta^2 W = \frac{1}{2}G\gamma^2 + \frac{m-2}{8}\gamma^2 (S_1^0 + S_3^0) + \frac{1}{2}(S_1^0 u_{3,1}^2 + S_3^0 u_{1,3}^2) \quad (6)$$

This equivalence yields:

$$m = \frac{2(S_3^0 / S_1^0) - 2}{(S_3^0 / S_1^0) + 1} \quad (7)$$

It follows that, for small-strain incremental continuum analysis of an initially stressed homogenized layered or fiber-reinforced medium very soft in shear, a constant small-strain shear

modulus G can be used if, and only if, the formulation corresponding to the finite strain tensor of parameter m given by Eq. (7) is used. To be able to apply the standard finite element algorithm, which is associated with $m=2$ and is used in all the commercial finite element programs at present, the small-strain shear modulus G must be transformed, at each stage of loading, according to Eq. (4).

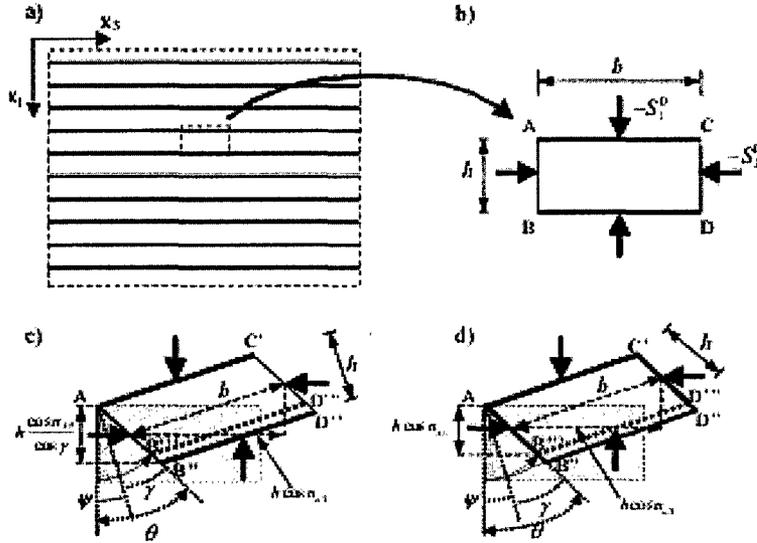


Figure 10: Fiber reinforced material biaxially loaded: a) uni-directional fiber reinforced material; b) geometry of a representative volume element; c) Shear deformation for uni-directional reinforcement; and d) shear deformation for orthogonal reinforcement.

Initial Postbuckling of Sandwich Structures

The initial postbuckling characteristics of sandwich structures have been explored in order to understand the effect of imperfection sensitivity. To this end a homogenized sandwich column has been analyzed in finite strain under the following kinematic assumption for the displacement field:

$$U(X, Z) = U_0(X) - Z \frac{d\psi_0}{dX} \quad W(X, Z) = W_0(X) + Z \frac{dU_0}{dX} \quad (8)$$

Where X, Z denote Lagrangian coordinates, U, W are the displacements of a 2D continuum in directions X and Z respectively, ψ is the angle of rotation of the cross section, and subscript 0 refers to quantity describing the displacement of the center line of the beam. After substituting the above expressions into the Doyle-Ericksen tensor, the potential energy can be written as:

$$\delta^2 W = \int_0^L \int_A \left[\Sigma_{XX}^{(m)} \epsilon_{XX}^{(m)} + \Sigma_{ZZ}^{(m)} \epsilon_{ZZ}^{(m)} + 2\Sigma_{XZ}^{(m)} \epsilon_{XZ}^{(m)} \right] dA dX + P \int_0^L \frac{dU_0}{dX} dX \quad (9)$$

where $\Sigma_{ij}^{(m)}$ denotes the stress measure conjugate to the strain measure for the given value of m .

The governing equations of the initial postbuckling problem have been derived by applying Koiter's approach, which is based on introducing a perturbation ϵ in the expression of the governing variables of Eq. (9) and imposing the condition of vanishing first variation of the potential energy. After a rather long derivation, one gets a complex formula to describe the imperfection sensitivity, which is seen to depend on the material stiffnesses, parameter m and the

boundary conditions. The results for a beam with aspect ratio $L/h=5$ are plotted in Figure 11 (on the left). The figure shows that for certain values of the parameters the imperfection sensitivity appears (white region in the figure), causing the structure to reach a maximum load less than the bifurcation load and then soften.

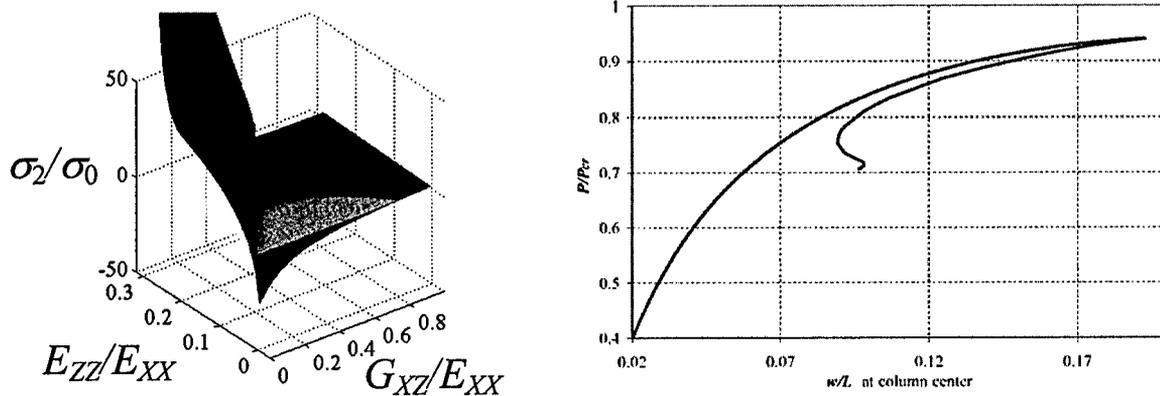


Figure 11: Region of imperfection sensitivity for a column with $L/h=5$ (left) and results of a finite element analysis for a column with $L/h=5$, $E_{zz}/E_{xx}=0.045$, $G_{xz}/E_{xx}=0.16$ (right).

In order to clarify the implications for FE analysis of sandwich structures, a column of aspect ratio $L/h=5$, $E_{zz}/E_{xx}=0.045$ and $G_{xz}/E_{xx}=0.16$ has been analyzed. The result of the analysis is shown in Figure 11 (on the right). The analysis provides a maximum load that is extremely close to the prediction of the formulas, confirming the validity of the analytical approach.

5. Revision of structural reliability concepts for quasibrittle structures taking into account size dependence of pdf

The greatest error in design is probably caused by the safety factors, which are still largely empirical, and any improvement is bound to bring about greater benefits than any improvements in deterministic computational modeling. Investigations during the last year revealed the need for a major revision of reliability concepts used in the of quasibrittle heterogeneous structures, such as large load-bearing fiber-composite parts for ships or aircraft.

The main phenomenon, previously unappreciated, is that the not only the mean nominal strength of structure but also its coefficient of variation and especially the far-out pdf tail depends on structure size, and that even the type of probability distribution depends on structure size. While ductile failure occurs simultaneously along the failure surface and is characterized by absence of size effect and Gaussian distribution of structural strength, quasibrittle failures propagates, exhibits a strong size effect and follows at large sizes extreme value statistics of weakest-link model, which leads to Weibull distribution of structural strength (provided that failure occurs at macro-crack initiation from cracking zone).

The mechanical-statistical assessment of quasibrittle failure risk and of the size effect on safety factors must be based on the material nano-scale. In the design of ships as well as other structures, one must ensure an extremely low failure probability such as 10^{-6} . How to do that has been adequately understood only for the limiting cases of brittle or ductile structures. Developed has been a theory to do that for the transitional class of quasibrittle structures, having brittle constituents and characterized by nonnegligible size of material inhomogeneities. It was shown that the probability distribution of strength of the representative volume element (RVE) of material is governed by the Maxwell-Boltzmann distribution of atomic energies and the stress dependence of activation energy barriers. This distribution is statistically modelled by a hierarchy of series and parallel couplings. It consists of a broad Gaussian core having a grafted far-out power-law tail with zero threshold and amplitude depending on temperature and load duration. With increasing structure size, the Gaussian core shrinks and Weibull tail expands according to the weakest-link model for a finite chain of RVEs. The model captures experimentally observed deviations of the strength distribution from Weibull distribution, and of the mean strength scaling law from a power law. These deviations can be exploited for verification and calibration. The proposed theory will increase the safety of composite parts ships (as well as aircraft) and allow designs closer to the safety margin.

To describe structural strength distribution based on the chain-of-bundles model, a composite pdf with Weibull tails grafted on a Gaussian core is introduced. For the small-size limit, the core is totally Gaussian, and for large-size limit totally Weibull. In between, the grafting point moves inward and the Gaussian core shrinks with increasing size. This causes that the distance from the mean to a point of tolerable failure probability (such as 10^{-7}) nearly doubles as the size of quasibrittle structure increases.

Consequently, the understrength part of the safety factor used in design should be made size dependent. So must the Cornell and Hasofer-Lind reliability indices for FORM, which are used to estimate failure probability of structures.

PI's Publications Supported Partly or Fully by This Grant

Books

Bazant, Z.P., (2005). "Scaling of structural strength", 2nd revised edition, Dover, New York.

Refereed Journal Articles

1. Bazant, Z.P., Zhou, Y., Novak, D., and Daniel, I.M. (2004). "Size effect on flexural strength of fiber-composite laminate." *J. of Engrg. Materials and Technology ASME* 126 (Jan.), 29--37.
2. Carol, I. (2004), Jirasek, M., and Bazant, Z.P.. "A framework for microplane models at large strain, with application to hyperelasticity." *Int. J. of Solids and Structures* 41, 511--557.
3. Bazant, Z.P., and Di Luzio, G. (2004). "Nonlocal microplane model with strain-softening yield limits." *Int. J. of Solids and Structures* 41 (24-25), 7209-7240.
4. Bazant, Z.P. (2004). "Scaling theory for quasibrittle structural failure." *Proc., National Academy of Sciences* 101 (37), 14000-14007 (inaugural article).

5. Bazant, Z.P. (2004). "Probability distribution of energetic-statistical size effect in quasibrittle fracture." *Probabilistic Engineering Mechanics* 19 (4), 307-319.
6. Bazant, Z.P., and Beghini, A. (2004). "Sandwich buckling formulas and applicability of standard computational algorithm for finite strain." *Composites: Part B* 35, 573-581.
7. Bazant, Z.P., and Yavari, A. (2005). "Is the cause of size effect on structural strength fractal or energetic-statistical?" *Engrg. Fracture Mechanics* 72, 1-31.
8. Guo, Z., and Bazant, Z.P. (2004). "Theoretical modeling and scaling." Sec. 4, pp. 584-592 and 596-600 in chapter on "Micro- and nanomechanics" by B.C. Prorok, Y. Zhu, H.D. Espinosa, Z. Guo, Z.P. Bazant, Y. Zhao and B.I. Yakobson, Vol. 5, pp. 555-600 in *Encyclopedia of Nanoscience and Nanotechnology*, H.S. Nalva, ed., American Scientific Publishers, Stevenson Ranch, CA.
9. RILEM Technical Committee QFS (chaired by Z.P. Bazant)(2004). "Quasibrittle fracture scaling and size effect---Final report." *Materials and Structures* 37, 547--586.
10. Cervenka, J., Bazant, Z.P., and Wierer, M. (2005). "Equivalent localization element for crack band approach to mesh-sensitivity in microplane model." *Int. J. for Numerical Methods in Engrg.* 62 (5), 700-726.
11. Bazant, Z.P., and Beghini, A. (2005). "Which formulation allows using a constant shear modulus for small strain-buckling of soft-core sandwich structures?" *J. of Applied Mechanics ASME* 72 (Sept.), 785-787.
12. Di Luzio, G., and Bazant, Z.P. (2005). "Spectral analysis of localization in nonlocal and over-nonlocal materials with softening plasticity or damage." *Int. J. of Solids and Structures* 42, 6071-6100.
13. Bazant, Z.P., and Beghini, A. (2006). "Stability and finite strain of homogenized structures soft in shear: sandwich or fiber composites, and layered bodies." *Int. J. of Solids and Structures* 43, 1571-1593.
14. Bazant, Z.P., and Pang, S.-D. (2006). "Mechanics based statistics of failure risk of quasibrittle structures and size effect on safety factors." *Proc. of the National Academy of Sciences* 103 (25), 9434-9439.
15. Beghini, A., Bazant, Z.P., Waas, A.M., and Basu, S. (2006). "Postcritical imperfection sensitivity of sandwich or homogenized orthotropic columns soft in shear and in transverse deformation." *Int. J. of Solids and Structures* 43, 5501-5524.
16. Bazant, Z.P., Zhou, Y., Daniel, I.M., Caner, F.C., and Yu, Q. (2006). "Size effect on strength of laminate-foam sandwich plates", *J. of Engrg. Materials and Technology ASME* 128 (3), 366-374.

Refereed Journal Articles in Press:

17. Bazant, Z.P., and Pang, S.-D. (2006). "Activation energy based extreme value statistics and size effect in brittle and quasibrittle fracture". *J. of the Mechanics and Physics of Solids* 54, in press.
18. Bayldon, J., Bazant, Z.P., Daniel, I.M., and Yu, Q. (2006). "Size effect on Compressive Strength of Laminate-Foam Sandwich Plates." *J. of Engrg. Materials and Technology ASME* 128, in press.
19. Bazant, Z.P., Vorechovsky, M., and Novak, D. (2006). "Asymptotic prediction of energetic-statistical size effect from deterministic finite element solutions." *J. of Engrg. Mech. ASCE* 128, in press.
20. Bazant, Z.P., and Yu, Q. (2006). "Size Effect on Strength of Quasibrittle Structures with Reentrant Corners Symmetrically Loaded in Tension." *J. of Engrg. Mech. ASCE* 128, in press.

In Conference Proceedings:

- P1. Vorechovsky, M., Bazant, Z.P., and Novak, D. (2005). "Procedure of statistical size effect prediction for crack initiation problems." Proc. (CD) 11-th Int. Conf. on Fracture (ICF-11, held in Turin, Italy), A. Carpinteri, ed., Paper 40-6-1, pp. 1-6.
- P2. Bazant, Z.P., and Pang, S.-D. (2005). "Revision of Reliability Concepts for Quasibrittle Structures and Size Effect on Probability Distribution of Structural Strength." Safety and Reliability of Engrg. Systems and Structures (Proc., 8th Int. Conf. on Structural Safety and Reliability, ICOSSAR 2005, held in Rome), G. Augusti, G.I. Schueller and M. Ciampoli, eds., Millpress, Rotterdam, pp. 377-386.
- P3. Bazant, Z.P., Vorechovsky, M., and Novak, D. (2005). "Role of deterministic and statistical length scales in size effect for quasibrittle failure at crack initiation." *ibid.*, pp. 411-415.
- P4. Bazant, Z.P., and Pang, S.-D. (2005). "Effect of size on safety factors and strength of quasibrittle structures: Beckoning reform of reliability concepts." Proc., The Structural Engineering Convention (SEC 2005), J.M. Chandra Kishen & D. Roy, eds., Indian Institute of Science, Bangalore, India, pp. 2-20.
- P5. Bazant, Z.P., and Grassl, P. (2006). "Size effect of cohesive delamination fracture triggered by sandwich skin wrinkling." Marine Composites and Sandwich Structures. (Proc., ONR Solid Mechanics Program Annual Review Meeting, Y.D.S. Rajapakse, ed., University of Maryland, pp. 12--20.